

Dynamic optical correlation using localized holography

Arash Karbaschi, Omid Momtahan, and Ali Adibi

School of Electrical and Computer Engineering, Georgia Institute of Technology, Atlanta, Georgia 30332, USA

Received October 9, 2006; revised December 14, 2006; accepted December 16, 2006;
posted January 3, 2006 (Doc. ID 75879); published February 15, 2007

A new technique for optical correlation using gated holographic recording is demonstrated. Several persistent holograms are localized within separate slices as close as $33\ \mu\text{m}$ apart along the crystal. Individual holograms can be dynamically erased and rerecorded with no need to refresh all other recorded holograms. Experimental results showing the correlation capability, cross talk, shift invariance, and dynamicity of the localized holographic correlator demonstrate unique performance and capabilities for these correlators.

© 2007 Optical Society of America

OCIS codes: 070.4550, 090.7330.

Optical signal processing and pattern recognition have been appreciated since the complex spatial filtering work by VanderLugt in 1964.¹ The multiplexing advantage of volume holography has made it a significant method to be employed in optical pattern recognition. Most of the holographic correlators are based on the angular multiplexing technique.² Recently, we introduced the theoretical framework of a new class of holographic correlators³ based on the localized recording technique,⁴ which can be implemented using a gated holographic recording scheme such as two-center recording in doubly doped LiNbO_3 crystals.⁵ By use of gated holography, the recording and erasure of the holograms are possible only in the presence of a gate beam. A simple demonstration of the localized holographic correlator (LHC) is shown in Fig. 1. By shaping the gate beam to form a thin slice within the crystal, the hologram is localized within the volume of that slice [Fig. 1(a)]. The recording beams affect only the sensitized slice and have a negligible effect on other holograms in other slices. Therefore, individual patterns can be dynamically recorded and erased in separate slices of the recording medium. Furthermore, because the absorption of the signal beam as propagating through the crystal is negligible outside the sensitized slice, it is possible to use long crystals to extend the capacity of the LHC. During the correlation phase, the signal beam corresponding to the pattern under investigation propagates through the crystal and is correlated with all the holograms stored in all slices along the crystal. The correlation beams are diffracted toward the detector array right next to the crystal [Fig. 1(b)], with no requirement of a collecting lens after the hologram. This makes the LHC more compact than the conventional holographic correlators. Using theoretical simulations, it is shown that the overall performance of LHCs in terms of cross talk, shift invariance, and capacity is better than that of the conventional correlators.³

In this Letter, we present the first experimental results showing the correlation capability, cross talk, shift invariance, and dynamicity of the LHC. Figure 2 is a schematic illustration of the LHC experimental setup. The 532 nm expanded laser beam from a diode-pumped solid-state laser illuminates a spatial

light modulator (SLM), which modulates the signal beam with the information of the recorded and correlated patterns in recording and correlation phases, respectively. The DC component of the signal beam is then filtered out at the origin of the Fourier plane of a 4- f imaging system comprising two confocal lenses, F1 and F2. All of the correlated patterns have a DC component. This is caused by the SLM's being an intensity modulator, producing a nonzero field average for each pattern. Eliminating this common part of the spatial spectrum of the patterns significantly improves the contrast of the correlation process. All the diffraction orders of the SLM, except the zeroth order, are also blocked at the focal plane of lens F1. The magnification ratio of the 4- f system is 1:1.5. The filtered pattern is then Fourier transformed by lens F3 at the entrance facet of the holographic crystal. The focal lengths are chosen to have half of the Fourier transform pattern fit to the crystal width (L_X in Fig. 2). This doubles the spatial bandwidth of the system while maintaining the same crystal width.

The reference and the UV gate (wavelength 404 nm) beams are coaligned and are focused by the cylindrical lens CL1 inside the crystal at the same location, where they form two overlapping slices of light that define the recording slice. Before merging of these two copropagating beams, they are filtered and shaped like one-dimensional Gaussian beams by two separate sets of confocal cylindrical lenses [(CL2, CL3) for the reference and (CL4, CL5) for the UV] and slits. The slits remove the fringes that would appear around the main light slice. This significantly reduces the cross talk between adjacent slices. Also, the holograms can be selectively recorded and erased

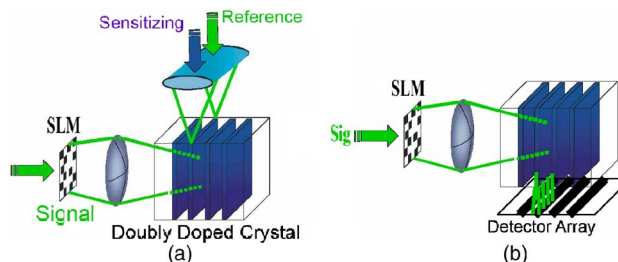


Fig. 1. (Color online) Localized holographic correlation steps: (a) recording, (b) correlation.

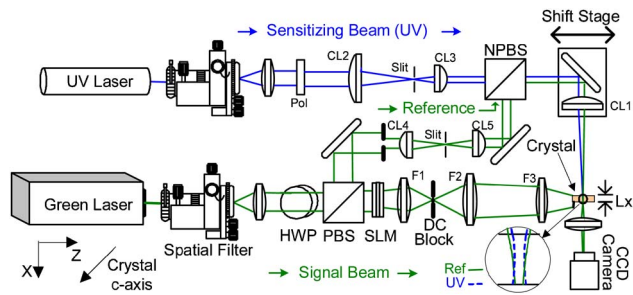


Fig. 2. (Color online) LHC experimental setup. HWP, half-wave plate; PBS, polarizing beam splitter; NPBS, nonpolarizing beam splitter; F1–F3, Fourier transform lenses; CL, cylindrical lens; Pol, polarizer. Lens focal lengths: $f_1 = 20$ cm, $f_2 = 30$ cm, $f_3 = 12.5$ cm, $f_{CL1} = 5$ cm.

within select slices without erasing neighboring holograms. The beam waist diameters ($2w_0$) of the reference and UV Gaussian beams are $18\ \mu\text{m}$. The full width of the UV beam within the crystal defines the slice thickness. The waist of the UV beam occurs in the center of the entrance and exit facets of the crystal. The waist of the reference beam is located at the exit facet of the crystal, where the detector array is planned to be attached (or placed in close proximity). The location of the two overlapping beams (i.e., reference and UV) along the crystal is controlled by a precision translation stage, which shifts the focusing cylindrical lens CL1. For simplicity, in all the demonstrations of the LHC in this Letter the diffracted correlation signal at the exit facet of the crystal is imaged onto a CCD camera by a lens, rather than being collected by a detector array.

The recording medium is a 45° -cut congruently grown $\text{LiNbO}_3:\text{Fe}:\text{Mn}$ crystal doped with 0.15 wt.% Fe_2O_3 and 0.02 wt.% MnO . The crystal dopant contents are optimized to acquire high sensitivity and high dynamic range ($M/\#$ parameter) at the same time.⁶ The crystal is annealed at 1070°C in oxygen atmosphere for 48 h. The crystal width is $L_x = 1.6$ mm. The employed SLM has a resolution of 1024×768 and a pixel pitch of $14\ \mu\text{m}$ in both the x and y directions. The applied patterns are pages of random dark and bright 2×2 superpixels as zeros and ones. Because of the 1:1.5 magnification ratio of the 4- f imaging system, the effective pixel size of the recorded pattern is $p = 2 \times 14 \times 1.5 = 42\ \mu\text{m}$.

To investigate the cross talk in LHCs, we used the experimental setup in Fig. 2 to record localized holograms of random patterns in seven slices $33\ \mu\text{m}$ apart from each other. Comparing the $33\ \mu\text{m}$ slice distances with the width of the holograms (about $18\ \mu\text{m}$) it is notable that we have added a buffer space between adjacent holograms to reduce cross talk. To the best of our knowledge, the $33\ \mu\text{m}$ distance between the adjacent slices is the smallest reported to date for localized holography. To study the cross talk in the worst case scenario, we left the center slice blank (i.e., no hologram recorded) and used the same pattern for all the other six holograms. The holograms were then read by the same pattern used for recording. The diffracted signals at all seven slices are shown in Fig. 3(a). Because there is no ho-

logram recorded within the gap at the center slice in Fig. 3(a), the power collected at this slice is initiated from the tails of the diffraction profiles of the neighboring holograms and small scatterings, which is defined as cross talk.³ Figure 3(a) clearly shows the negligible cross talk in LHCs. The cross-talk noise-to-signal ratio (NSR), which is the ratio of the power at the location of the missing hologram to that at the adjacent peaks, is about -20 dB. We repeated the above experiment with the same pattern used for six holograms, but instead of leaving the center slice blank, we used a different random pattern for recording a hologram there. The holograms were then read by the same pattern used for recording the six surrounding holograms. The diffracted signals at all the seven slices are shown in Fig. 3(b). The collected power at the middle slice represents the cross-correlation of the reading pattern and that used for recording of the middle hologram plus the cross talk caused by diffraction from adjacent holograms at the middle slice. Comparing Figs. 3(a) and 3(b), it is observed that the amount of power at the location of the unmatched hologram [in the middle slice in Fig. 3(b)] is about the same as that at the location of the blank slice [in the middle slice in Fig. 3(a)]. One can conclude that the system does the cross-correlation well with good discrimination. It is notable in Fig. 3 that the strength of the six holograms is decreasing from left to right. The holograms have been recorded in order from right to left. During recording of each hologram, the signal beam reads previously recorded holograms, which partially erases them. Partial loss of persistence while reading with green light explains this effect.⁷ Instead of equal recording times for all of the holograms, a schedule can be calculated for the recording times based on the recording and erasure time constants, which results in equal strengths of the recorded holograms.⁸

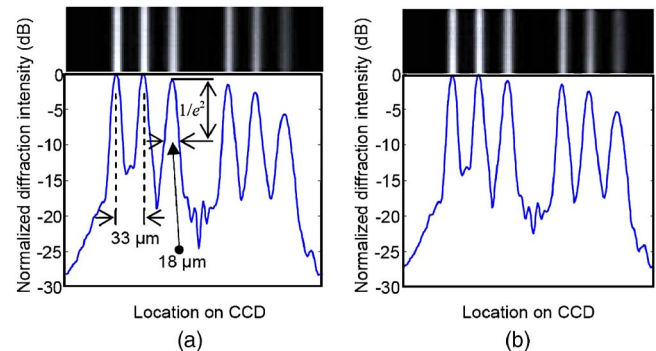


Fig. 3. (Color online) Diffraction signals from six localized holograms recorded with the same random pattern as the one reading them. The pictures on top of the curves are the images of the diffraction signals at the CCD in Fig. 2. The holograms were recorded in order from right to left, each for 180 s with no presensitizing. The intensities of the recording reference and signal beams and that of the UV beam are 300 , 300 , and $40\ \text{mW}/\text{cm}^2$, respectively. Two cases are demonstrated: (a) no hologram is recorded in the middle slice, and (b) a hologram with a totally uncorrelated random pattern is recorded in the middle slice. In both (a) and (b) curves, the intensity values are normalized to the intensity value at the largest diffraction peak among all holograms in each case.

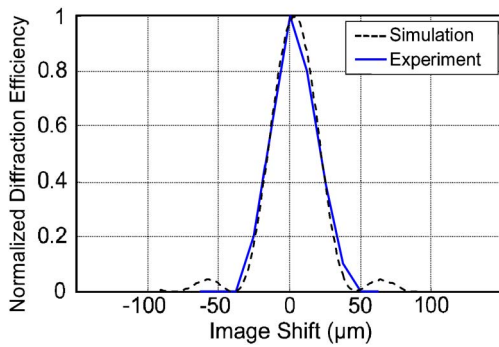


Fig. 4. (Color online) Shift invariance of the LHC, simulation and experiment. The in-plane shift (in the x -direction in Fig. 2) is applied. The horizontal axis corresponds to the shift of the magnified pattern behind lens F2 in Fig. 2. The pixel pitch of the magnified pattern is $42 \mu\text{m}$.

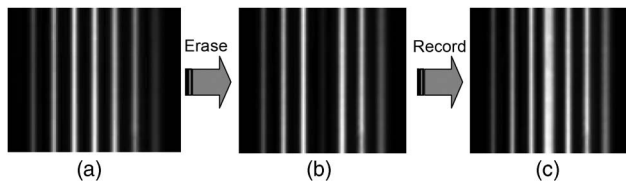


Fig. 5. Dynamic recording/erasure in LHC. (a) Seven holograms are recorded in order from right to left. (b) The hologram at the center is erased by illuminating it with the UV and reference beams, and (c) the hologram at the center is rerecorded for 2 min. The recording and reading intensities are the same as those mentioned in the caption of Fig. 3.

Another important property of any correlator is shift invariance, which is defined as the minimum amount of the lateral shift of the matched reading pattern required to reduce the diffraction efficiency to zero.³ To study the shift invariance of the LHC, one hologram was recorded in one slice. The hologram was then read by the same pattern used for recording but the pattern was shifted by different amounts on the SLM. The in-plane shift was applied (i.e., in the x -direction in Fig. 2). The diffraction efficiency was measured per each shift value. Figure 4 shows the diffraction efficiency, normalized to the diffraction efficiency at no shift, as a function of the in-plane shift in the reading pattern. The shift invariance approximately equals the effective pixel pitch: $42 \mu\text{m}$. To examine the validity of this result, we calculated the in-plane shift invariance with the parameters of the experiment using the formulation in Ref. 3. The theoretical results are also shown in Fig. 4. It is observed that the simulation and experimental results agree well. Both the simulation and experimental curves show asymmetry in the response to the in-plane shift, because of the asymmetry of the grating vector (directed along the c -axis) with respect to the z -axis (Fig. 2).

A unique advantage of the LHC is the possibility of dynamic modification of the pattern database. To investigate this effect, we recorded seven holograms with the same pattern. The holograms were then read by the same pattern. The diffracted signals are shown in Fig. 5(a). The recording times varied from 15 min for the right-side hologram (first recorded),

exponentially reduced from one slice to another, to 2 min for the left-side one (last recorded) with no pre-sensitizing phase. We then erased the middle hologram by illuminating the middle slice with the UV beam and the reference beam for 20 min without changing their intensities. After erasure, the holograms were read by the recording pattern, and the diffracted signal is shown in Fig. 5(b). The erasure time was selected properly so that the diffraction efficiency of the middle hologram was significantly reduced. The erasure time is larger than the typical recording time because of Bragg-matched erasure. The erased hologram was then rerecorded for 2 min. Then, the holograms were read by the recording pattern and the diffracted signals are shown in Fig. 5(c). The neighboring holograms remained intact. The results shown in Fig. 5 prove that the recorded holograms within the recording medium can be selectively erased and replaced with other desired holograms. Therefore, it is possible to dynamically modify the patterns stored in the LHC with no need to refresh all of the stored patterns. Note that the diffracted signal from the middle hologram after rerecording appears wider than those of the six surrounding holograms. We think this is caused by the nonuniformity of the refractive index at the location of the middle slice after erasing by the UV and reference beams, which scatters the reference beam in the rerecording step. Investigation is underway to minimize this effect.

In conclusion, we presented what is to our knowledge the first experimental demonstration of a LHC system with good correlation performance. We demonstrated dynamic recording and erasure of localized holograms $33 \mu\text{m}$ apart from each other, which is to date the smallest reported distance between localized recorded holograms of which we are aware. The cross talk and shift invariance of the LHC are within acceptable range for the optical correlators. The unique feature of the LHC, the dynamic pattern modification, in principle, was demonstrated by erasing one hologram among a few holograms and rerecording it with no effect on the surrounding holograms.

This work was supported by Air Force Office of Scientific Research under contract FA9550-05-1-0438 (G. Pomrenke). A. Adibi's e-mail address is adibi@ece.gatech.edu.

References

1. A. B. VanderLugt, *IEEE Trans. Inf. Theory* **IT-10**, 139 (1964).
2. A. Pu, R. Denkwalter, and D. Psaltis, *Opt. Eng. (Bellingham)* **36**, 2737 (1997).
3. A. Karbaschi, O. Momtahan, A. Adibi, and B. Javidi, *Opt. Eng. (Bellingham)* **44**, 085802 (2005).
4. C. Moser, B. Schupp, and D. Psaltis, *Opt. Lett.* **25**, 162 (2000).
5. K. Buse, A. Adibi, and D. Psaltis, *Nature* **393**, 665 (1998).
6. O. Momtahan and A. Adibi, *J. Opt. Soc. Am. B* **20**, 449 (2003).
7. A. Adibi, K. Buse, and D. Psaltis, *Opt. Lett.* **25**, 539 (2000).
8. A. Adibi, K. Buse, and D. Psaltis, *Opt. Lett.* **24**, 652 (1999).